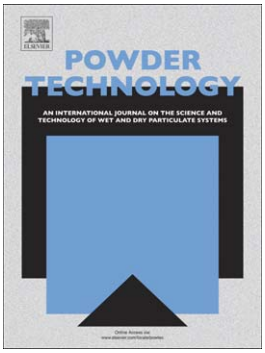

Powder distribution on powder injection moulding of ceramic green compacts using thermogravimetric analysis and differential scanning calorimetry

Leslie Poh, Christian Della, Shengjie Ying, Cindy Goh, Yun Li

PII: S0032-5910(17)31037-9
DOI: doi:10.1016/j.powtec.2017.12.078
Reference: PTEC 13067

To appear in: *Powder Technology*

Received date: 19 March 2017
Revised date: 17 December 2017
Accepted date: 28 December 2017

Please cite this article as: Leslie Poh, Christian Della, Shengjie Ying, Cindy Goh, Yun Li, Powder distribution on powder injection moulding of ceramic green compacts using thermogravimetric analysis and differential scanning calorimetry, *Powder Technology* (2018), doi:10.1016/j.powtec.2017.12.078

Title: Powder distribution on powder injection moulding of ceramic green compacts using thermogravimetric analysis and differential scanning calorimetry

Leslie Poh,[a,b] Christian Della,[b] Shengjie Ying,[a] Cindy Goh[b] and Yun Li[b,*)]

[a]*Dou Yee Technologies Pte Ltd, 113 Defu Lane 10, Singapore 539227*

[b]*School of Engineering, University of Glasgow, Oakfield Avenue, Glasgow G12 8LT, U.K.*

Abstract

Powder-binder separation during injection moulding causes defects such as cracking, warpage or anisotropic shrinkage during firing. In this paper, thermogravimetric analysis (TGA) and differential scanning calorimetry (DSC) that were previously used to analyse powder distribution within the green body for metal injection moulding are used for ceramics. TGA and DSC are used to characterise the mass loss and heat of fusion of the binder system, silicon nitride feedstock and test-bars. TGA can measure the volume fraction of powder in green parts directly with 1.76 vol% difference from nominal volume fraction and variations up to 0.177 vol%. The DSC empirical model predicted volume fraction of powder in green parts with 1.76 vol% difference from nominal volume fraction and variations up to 1.710 vol%. Using rule of mixture, it over predicted volume fraction of powder in green parts by 6.78 vol% from nominal volume fraction and with variations up to 2.510 vol%.

1. Introduction

Powder injection moulding (PIM) is a combination of plastic injection moulding and powder metallurgy processes such as compounding, moulding, debinding and sintering. Defects have been known to arise during any stage of the PIM process including poor dispersion of powder and binder during compounding, surface and structural defects from injection moulding, deformation and cracking during debinding and anisotropic shrinkage, cracking and warpage during sintering [1-9]. These defects that emerges during moulding cannot be resolved in the latter process [3, 10, 11]. Separation between powder and binder has been identified as one of the causes of such defects and it occurs due the

*Author to whom correspondence should be addressed. Electronic mail: Yun.Li@glasgow.ac.uk

high shear rates during injection moulding has been reported to be the main cause of inhomogeneity in green compacts [9]. This form of separation that is cause by imperfection forming process is known as phase segregation. Another form of separation between the powder and binder has been known to occur during compounding of powder and binder mixture to form the feedstock. Homogeneous distribution between powder and binder is highly desirable to prevent any defects. Inhomogeneous distribution between powder and binder in green compacts are hard to identify and this uneven distribution causes thermal expansion to vary with position and direction [12]. The separation of powder and binder can be evaluated by measuring the density, specific heat, thermal conductivity, heat of fusion, weight loss after binder burnout, electrical conductivity, rheology and microscopic examination [13-17]. These methods measure the solid loading which is the equivalent to the volume fraction of powder in the specimen.

Studies on powder injection moulding process that uses numerical models and simulation focuses on the moulding filling stage of injection moulding [18-20]. These studies showed that the quality of green compact is dependent on the injection moulding process parameters such as injection pressure, holding pressure, temperature of the feedstock, mould temperature, filling time, cooling time, feedstock thermal and rheological properties. The results from these optimisation and simulation studies need to be validated using test data. Therefore, powder distribution analysis method that measures the powder content within a green body is crucial to the development works of PIM. Based on the literatures, several methods have studied the use of X-ray computed tomography, thermogravimetric analysis (TGA), differential scanning calorimetry (DSC), pycnometer, Archimedes' principle for powder distribution analysis of ceramic and metal green bodies [17, 20-23].

Authors have shown that the TGA and DSC can be used to determine binder content of powder-binder mixtures, the homogeneity of metal-powdered feedstock [17]. The sensitivity of using the TGA, DSC and pycnometer to measure the solid volume of metal-powdered feedstock was compared and it showed that these methods can be used to measure the segregation effects within the feedstock. TGA method can also be used to detect the point to point distribution and segregation of metal powder in green parts as demonstrated [17]. The additional benefits of using the TGA and DSC is that they can be used to determine other process parameters useful for the debinding and injection moulding process. By observing the weight loss of binders during binder burnout in a TGA, thermal debinding process parameters such as holding temperature and duration can be determined and refined [24, 25]. The residual weight from the TGA after burnout will determine the powder content in the specimens. Any phenomenal weight gains that may occur will be recorded during the experiments which would assist in the determination of optimal process parameters for solvent and

thermal debinding. The thermal properties such as specific heat and heat of fusion of metal-powdered feedstock have been demonstrated to be determined by the volume fraction of powder and binder [17, 26]. Using the DSC, softening points, heat of fusion, specific heat capacity of the binders and feedstock can be determined, and this can be used to identified suitable compounding and moulding temperatures [1].

To the authors' best knowledge, the use of TGA and DSC to measure the powder distribution of powders in powder injection moulding has only been done on metal powders. The use of these method has yet to be considered and presented on ceramic powders in injection moulded green bodies. This study aims to investigate use of TGA and DSC to determine the powder distribution and segregation of silicon nitride powder within injection moulded test-bars. The objectives are:

1. develop TGA and DSC based methods to investigate the powder distribution in ceramic green compacts;
2. develop empirical models to determine the powder content within the material for powder distribution analysis; and
3. analyse and compare TGA and DSC as measurement methods to determine powder distribution analysis of ceramic green bodies

2. Materials and methods

2.1. Material preparation

Fig. 1. (a) Binder system and (b) Si_3N_4 feedstock

A multi-component binder system (Binder) and a silicon nitride feedstock (Feedstock) are used in this study, as shown in Figs. 1(a) and 1(b). The binder system consists of high density polyethylene (HDPE) with melt index of 18 g/10 min and density of 0.955 g/cc, paraffin wax (PW) with melting point ranging 58 – 60 °C and stearic acid (SA). Silicon nitride (Si_3N_4) powder used had 99.9% purity, as α-phase crystalline structure and particle size of 0.6 - 0.8 µm, Fig. 1(c). The silicon nitride powder was dope with magnesium oxide (MgO) powders with 99.9% purity and yttrium oxide (Y_2O_3) powder with 99.95% purity, average particle size (d_{50}) of 0.8 µm and specific surface area (BET) 10 – 16 m^2/g. The composition of Binder and Feedstock, as shown in Table 1, were compounded separately using a IKA HKV-10 vertical kneading machine at temperatures ranging from 140 °C to 160 °C and a rotor speed of 15 to 40 rpm. Vacuum de-airing was used to ensure homogeneity in the feedstock. The homogeneity of the feedstock can be determined by measuring the variation in density using a gas pycnometer [17]. Pycnometer density experiment were carried out on a Micromeritics AccuPyc II 1340 Gas Pycnometer using helium gas. Three tests with total mass ranging from 2 to 7 g were carried on both Binder and Feedstock. The gas pycnometer determined variations/standard deviation in density of 0.0004 and

0.0038 in binder system and silicon nitride feedstock respectively, as shown in Table 1. The low variations in densities shows that binder system and powders were homogeneously mixed through the compounding process. With the average measured density of powders and binder system, the volume fraction of powders can be determined using the rule of mixture.

Table 1

Composition and density of binder system and silicon nitride feedstock.

Specimen	Si_3N_4 + MgO + Y_2O_3 vol% (wt%)	HDPE vol% (wt%)	PW+ SA vol% (wt%)	Theoretical Density (g/cm^3)	Measured Density (g/cm^3)	Measured Powder Volume Fraction (vol%)
Binder	-	51.37 (52)	48.63 (48)	0.9301	0.9241	-
Feedstock	45.08 (74)	28.21 (13.52)	26.71 (12.48)	1.9645	1.9633	45.16

Silicon nitride test-bars (Testbar), as shown in Fig. 2(a), were manufactured using an injection moulding machine (Engel, ES 200/45 HLS) with barrel temperature of 185 °C, mould temperature of 110 °C, injection speed ranging from 70 to 90 mm/s and injection pressure of 150 bar. The test-bars had dimensions of 60 × 12 × 3.5 mm. These test-bars were divided into 2 by 5 sections, upper and lower sections denoted by (A) and (B) and 5 smaller sections denoted from 1 to 5 as shown in Fig. 2(b). Smaller pieces of the specimen were cut out for the TGA and DSC test. A digital microscope, Keyence VHX-5000, was used to observe the surface area of the test-bars. Microscopy imaging of the silicon nitride test-bars in areas of the "1" near the gate shows surface defects, as shown in Fig. 2(c) and the areas in "3" shows no visible defects as shown in Fig. 2(d). Despite having a homogeneous feedstock, separation between the powder and binder still occurred during the injection moulding process. EDX can be combined with SEM to evaluate the element distribution of the main powder on the surface of the green body but it would not be able to quantify the localised effect of the separation [27].

Fig. 2. (a) Si_3N_4 test-bar and (b) schematic diagram for powder distribution study. (c) Microscopy imaging at area "1" and (d) at area "3".

2.2. Measurements

The TGA experiments were performed using a TA Instrument Q500 to determine the weight loss of the Binder, Feedstock and Testbar in a ramp temperature of 10 °C/min with N_2 purge gas flow rate of 90 mL/min over a temperature range from ambient temperature to 700°C. 100 µL platinum pans were used for the experiments. Thermal and

mechanical data were collected at a sampling rate of 2 points/s. TGA test were carried out on 5 samples of Binder, Feedstock and Testbar with weight range of 8 – 17 mg, 23 – 47 mg and 26 – 111 mg respectively. The DSC experiments were performed using a TA instrument Q100 to determine the heat flow of the Binder, Feedstock and Testbar at ramp temperature of 5 °C/min with N_2 purge gas flow rate of 50 mL/min over a temperature range from ambient temperature to 200 °C. Hermetic aluminium pans and lids were used for this experiment. Thermal data were collected at a sampling rate of 2 points/s. DSC tests were carried out on 5 samples of Binder, Feedstock and Testbar with weight range of 2.1 - 3.9 mg, 2.1 - 8.8 mg and 1.9 - 11.3 mg.

2.3. Methodology

With the TGA experiments, the powder content in the Feedstock or Testbar is determined by the remaining weight fraction of specimens. The volume fraction of powder is then determined using the rule of mixture and measured densities of powder and binder system. The TGA would reveal the weight loss curves and decomposition temperature of the binder components. This information can be used for the holding temperature during debinding of the green bodies. Thermal properties of a feedstock such as specific heat and heat of fusion can be predicted using the rule of mixture (ROM) [17, 28]. A ROM model could predict the heat of fusion of metal powdered feedstock with an accuracy of ±1 vol.% but it required a calibration curve and the heat of fusion of every binder component [17]. This is one of the two method that are presented in this paper to predict the volume fraction of powder with heat of fusion data. The assumption of this method is that the metal powder has lower heat of fusion as compared to the binders, hence an increase in solid loading would decrease the heat of fusion of the feedstock. This study investigates the heat of fusion data of the binder system instead of each binder component to determine the volume fraction of powder. The first model presented in (Equation 1) uses the ROM to predict the weight fraction of Binder in Feedstock based on the heat of fusion of the Binder and Feedstock. This model requires the use of a calibration curve determined by the heat of fusion of each binder component.

$$\Delta H_{feedstock} = \sum_i^n wt.\%_{binder,i} \times \Delta H_{binder,i} \quad (1)$$

The second model is an empirical equation (EMP) that was developed based on the experimental data. By considering the average heat of fusion of the binder system and silicon nitride feedstock and volume fraction of binder system in the silicon nitride feedstock (54.83 vol%) and binder system (100 vol%) that was determined based on the measured densities, a power-law model (Equation 2) is developed. This model requires the use of calibration curve determined by the heat of fusion of each binder component and the densities of each component in the feedstock.

$$\Delta H = 0.00198 vol.\%_{binder}{}^{2.4655} \quad (2)$$

Fig. 3 shows both models plotted in a graph. Equation 2 will allow the determination of volume fraction of binder system in the Si_3N_4 test-bars based on respective heat of fusion. By observing heat flow the melting points of the binder components in the Binder and Feedstock can be determined. This data can be used to determine the suitable mixing and injection moulding temperature for the silicon nitride feedstock. TA Universal Analysis software was used to calculate the heat of fusion in the specimens by integrating the area under the DSC peaks.

Fig. 3. Heat of fusion as a function of volume fraction of binder system in Feedstock based on experimental data, model 1 (ROM) and model 2 (EMP).

3. Results and discussions

3.1. Thermogravimetric Analysis (TGA)

Table 2

TGA results for Binder and Feedstock

Properties	Binder	Feedstock
Weight Range (mg)	8 – 17	23 – 47
Initial Degradation Temperature (IDT), T_{d5} (°C)	221	229
Maximum Derivative Rate (wt%/°C)	1.316	0.4
Maximum Derivative Rate (Scaled)	-	1.496
Final Residue (wt%)	-	73.2
Final Residue (vol%)	-	43.9

As shown in Fig. 4(a), the Binder and Feedstock revealed a two-stage weight loss curves due to the different decomposition temperature of the binder components. 5 wt% weight loss of binder system is considered as the initial degradation and the temperature for that weight loss for Binder and Feedstock is 221 °C and 229 °C, (Table 2). The first stage of decomposition ends when the weight loss starts to plateau at temperatures of 380 °C and 382 °C for Binder and Feedstock, respectively. The total weight loss for Binder and Feedstock at the respective temperatures are 48.6 wt% and 11.9 wt%. This corresponds to the weight fraction of paraffin wax (PW) and stearic acid (SA) in the Binder (48 wt%) and Feedstock (12.48 wt%). Second stage of decomposition for Binder and Feedstock occurred at 398 °C and 392 °C, respectively. The second stage of decomposition for Binder and Feedstock ends at 505 °C and 525 °C, respectively.

Binder was fully decomposed and Feedstock with a weight loss of 14.9 wt%. The weight fraction of high density polyethylene (HDPE) in Feedstock is 13.52 wt%. The weight fraction of the final residue in the Feedstock define the powder content in the feedstock. The weight loss of Feedstock at 185 °C where the injection moulding process was carried out was 0.3 wt% which is 1.1% of the binder system. A lower weight loss should be seen in the Testbar as binders are loss during injection moulding where small amounts of binders evaporated through the nozzle of the injection moulding barrel in to the atmosphere. However, it would not be as much as 0.3 wt% as the barrel of the injection moulding does not have purge gas flow environment like the TGA furnace. The derivative weight loss of the binder components in the Binder and Feedstock is shown in Fig. 4(b). The two-stage weight loss resulted in two derivative weight loss peaks. The derivative weight loss of Feedstock was scaled with respect to Binder by considering 100% weight loss to allow better comparison between Binder and Feedstock. Binder had its first peak at 291 °C with weight loss rate of 0.483 wt./°C and the second peak at 477 °C with weight loss rate of 1.316 wt./°C. The Feedstock had its first peak at 289 °C with weight loss rate 0.111 wt%/°C and the second peak at 473 °C with weight loss rate 0.4 wt./°C. When scaled to 100% the weight loss rate of Feedstock are 0.417 wt./°C and 1.496 wt./°C. The binder components (PW and SA) in the Feedstock that was not decomposed in the first stage have been burnout during the second stage. The final residual weight and volume fraction had variation/standard deviation of 0.191 and 0.240, respectively.

Fig. 4. (a) TG curves and (b) derivative TG curves of binder system and Si_3N_4 feedstock.

Table 3

TGA results for Testbar.

Properties	Testbar (1)	Testbar (2)	Testbar (3)	Testbar (4)	Testbar (5)
Weight (mg)	26-65	77-111	34-95	52-108	49-89
Average Volume% of Powders (vol%)	44.10	44.09	44.09	44.08	43.97
Variation/Standard Deviation (vol%)	0.112	0.0854	0.119	0.0961	0.0603

The Si_3N_4 test-bars were segmented based on the schematic diagram in Fig. 2(b) and TGA experiments were carried out on each of the section for all five Si_3N_4 test-bars. The final residual weight fraction, measured densities of powder and binder is then used to determine the volume fraction of powder in each section. Table 3 shows the weight range of each section, average volume fraction of powders and the variation in volume fraction of powder. Despite the wide weight range of specimens, the measured volume fraction of each section is within a close range of 43.97-44.10 vol% with highest variation of 0.119. This shows that the TGA can measure the volume fraction of powder content with wide range

of specimen weight. Fig. 5 shows a plot of the average volume fraction of powder in each section for part A and B. The points and error bars on Figs. 5-9 mark the volume fraction values and the variation of the measurements.

Fig. 5. Volume fraction of powders in Testbar from TGA a) Part A and b) Part B.

3.2. Differential Scanning Calorimetry (DSC)

Presented in Fig. 6, the DSC results of both the Binder and Feedstock showed two peaks where the first peak comprises of SA and PW and the second peak comprises of HDPE. The two peaks signify that the material goes through two endothermic reaction where each binder components are melting. The two distinct melting temperatures for the Binder are 59.7 °C and 123.3 °C. The two distinct melting temperatures for the Feedstock are 60.0 °C and 122.7 °C which is close to the Binder. The heat flow results of the Binder and Feedstock are studied and used to evaluate the weight fractions of the powder. The heat of fusion can be determined by integrating for the area under the curve for each peak. Five tests were carried out for the binder system and the Si_3N_4 feedstock. The Binder has an average heat of fusion of 73.28 J/g for the first peak and 95.97 J/g for the second peak which is a total of 169.25 J/g. The Si_3N_4 feedstock has an average heat of fusion of 14.52 J/g for the first peak and 23.99 J/g for the second peak which is a total of 38.51 J/g.

Fig. 6. Average heat flow curves of binder system and Si_3N_4 feedstock.

Table 4

Binder system volume fraction in Testbar based on ROM and EMP.

Method	Properties	Testbar (1)	Testbar (2)	Testbar (3)	Testbar (4)	Testbar (5)
-	Weight (mg)	3.5-11.1	3.6-7.7	1.9-11.3	3.5-9.7	2.7-7.8
ROM	Average Volume% of Powders (vol%)	49.79	50.88	52.04	51.55	50.72
	Variation/Standard Deviation (vol.%)	1.019	0.986	1.604	1.503	1.515
EMP	Average Volume% of Powders (vol%)	45.43	46.18	46.96	46.63	46.06
	Variation/Standard Deviation (vol.%)	0.699	0.674	1.092	1.023	1.035

With the same Si_3N_4 test-bar specimens that was used in the TGA, smaller pieces of each section were cut out and tested using the DSC based on similar experimental conditions as the binder system and Si_3N_4 feedstock. The weight range of each section, average volume fraction of powder and variations predicted based on ROM and EMP models are shown in Table 4. Fig. 7 and 8 show plots of the average volume fraction of powder and variation in each section for part (A) and (B) for ROM and EMP models. The ROM showed similar trends and variations as the EMP but higher magnitude

in volume fraction. Both methods are essentially empirical relations based off heat of fusion proportional to weight or volume fraction of binder in each section, hence they have similar trends.

Fig. 7. Volume fraction of powders in Testbar based on rule of mixture (ROM) a) Part A and b) Part B.

Fig. 8. Volume fraction of powders in Testbar based on empirical model (EMP) a) Part A and b) Part B.

3.3. Discussions

Fig. 9 show plots of the average volume fraction of powder and variation in each section for part (A) and (B) from the TGA and the DSC using the rule of mixture (ROM) and empirical (EMP) models. Table 5 presents the comparison of both methods and models on the variation of measured and predicted volume fraction and time taken for each test. The TGA results has a variation/standard deviation of 0.177 for the five experiments and up to 1.07 vol% difference from the nominal volume fraction of powder (45.08 vol%). The DSC results using the rule of mixture (ROM) has a variation/standard deviation of 2.510 for the five experiments and up to a 6.78 vol% difference and the empirical model (EMP) has a variation/standard deviation of 1.710 for the five experiments and up to a 1.78 vol% difference the nominal volume fraction of powder. The rule of mixture model (ROM) was intended to have a calibration curve with all the heat of fusion data for each component and measured densities of powder, binder and feedstock, thus it is not ideal in this application where only the heat of fusion was measured for the binder system. The empirical model (EMP) which able to use the measured heat of fusion of binder system and densities of powder, binder and feedstock to showed lower variations and closer to nominal volume fraction results as compared to the ROM model. From Fig. 5, the TGA results for part A and B shows slight decrease in the middle of the bar, this is backed by the low standard deviation of each section, in Table 5. The low deviation meant that the TGA can measure the powder content in feedstock and green bodies with good accuracy. The deviation of powder volume fraction across the test bars as shown in Table 3 is a good indication to the magnitude of segregation within a green body. Even though the DSC results has higher deviation compared to the TGA results, the results showed similar trend in terms of distribution. Similar to the previous works using the DSC on point to point analysis of powder distribution in green bodies, the DSC rule of mixture model does not have reasonable accuracy. However, the DSC empirical model has shown potential as a method to determine the point to point powder distribution in a green ceramic body and further works should be considered as the time taken for each test is much shorter than the TGA. If the ramp temperature used in the DSC is increased to 10 °C/min, it would shorten the time taken for each experiment and allowing the DSC to be more than 3 times faster at quantifying the powder distribution in a green body.

Fig. 9. Volume fraction of powders in Testbar from TGA, rule of mixture model (ROM) and empirical model (EMP), a) Part A and b) Part B.

Table 5

Comparison TGA and DSC

Measurement technique	Highest difference between nominal and measured value (vol.%)	Highest Variation/Standard Deviation in the sections (vol.%)	Ramp (°C/min)	Time taken (min)
Thermogravimetric analysis (TGA)	1.07	0.177	10	68.5
Differential scanning calorimetry (DSC)	6.78 (ROM) 1.76 (EMP)	2.510 (ROM) 1.710 (EMP)	5	36.8

4. Conclusions

Uniform distribution of powder content in an injection moulded green compact is important to prevent defects that will occur during debinding and sintering. Uneven distribution causes thermal expansion within the green compacts to vary, during thermal decomposition and densification the green compacts experiences anisotropic shrinkage which leads to cracking and warpages on the brown parts and sintered parts. The capability to measure powder distribution within the green compacts will allow early detection of defects and aid in the optimisation of the injection moulding process.

In this paper, the thermogravimetric analysis and differential scanning calorimetry were used to determine the volume fraction of powder in a green compact. The thermogravimetric analysis measured the mass loss after binder burnout of 10 different positions in a silicon nitride green compact. Using the final residual weight fraction and measure densities of powder and binder system, the volume fraction of powder can be determined. The method has a low variation of volume fractions of powder in feedstock (0.240 vol%) and sections of green compacts (0.177 vol%). The differential scanning calorimetry measured the heat of fusion of 10 different positions in a silicon nitride green compact. Rule of mixture and empirical models have been developed based on the DSC test results to determine the volume fractions of powder based on the measured heat of fusion. The two models relied on the heat of fusion of the binder system, feedstock and measured densities of powder and binder to determine the volume fraction. The rule of mixture model predicted a highest volume fraction of 52.04 vol% and a variation of 2.510 vol%. The empirical model predicted a highest volume fraction of 46.96 vol% and a variation of 1.710 vol%. Therefore, the empirical model developed in this study showed volume fractions closer to the nominal volume fraction (45.08 vol%) and lower variation as compared to the ROM model.

Based on the results of the study, the TGA measured the volume fraction of powders in feedstock and green compacts with the smallest variation. This makes the TGA suitable for quantifying the point to point powder fraction in green compacts for ceramic materials as well as quality control of the feedstock. The TGA method is also independent of the feedstock formulation as compared to the DSC methods that requires the use of calibration curve which requires heat flow data of binder components. The DSC empirical model showed reasonably accurate results with shorter test time.

Acknowledgements

This research is supported by the Economic Development Board of Singapore under grant, COY-15-IPP/130016, to Dou Yee Technologies Pte Ltd.

References

[1] R. Supati, N. H. Loh, K. A. Khor and S. B. Tor, "Mixing and characterization of feedstock for powder injection molding," *Materials Letters,* pp. 109-114, 2000.

[2] K. S. Roetenberg, R. Raman, C. I. Whitman, I. F. Snider Jr. and R. M. German, "Optimization of the mixing process for powder injection molding," in *Proceedings of the Powder Injection Molding Symposium*, York, 1992.

[3] T. Zhang, S. Blackburn and J. Bridgwater, "Debinding and sintering defects from particle orientation in ceramic injection molding," *Journal of Material Science,* vol. 31, no. 22, pp. 5891-5896, 1996.

[4] J. E. Zorzi, C. A. Perottoni and J. A. H. Jornada, "Method for the measurement of powder distribution in green ceramic bodies," *Journal of Material Science,* no. 22, pp. 107-109, 2003.

[5] M. J. Edirisinghe, "Fabrication of engineering ceramics by injection molding.," *American Ceramic Society Bulletin,* no. 70, p. 824, 1991.

[6] R. M. German and K. F. Hens, "Key issues in powder injection molding," *American Ceramic Society Bulletin,* no. 70, p. 1294, 1991.

[7] J. G. Zhang, M. J. Edirisinghe and J. R. G. Evans, "A catalouge of ceramic injection moulding defects and their causes," *Industrial ceramic,* no. 9, p. 72, 1989.

[8] M. R. Raza, F. Ahmad and M. A. G. R. Omar, "Defect Anaylsis of 316LSSduring the Powder Injection Moulding Process," *Defect and Diffusion Forum,* vol. 329, pp. 35-43, 2012.

[9] O. Weber, A. Rack, C. Redebach, M. Schulz and O. Wirjadi, "Micropowder injection molding: investigation of powder-binder separation using synchrotron-based microtomography and 3D image analysis," *Journal of Material Science,* no. 46, pp. 3568-3573, 2011.

[10] W. R. David, Modern Ceramic Engineering: Properties, Processing, and Use in Design, Florida: CRC Press, 2005.

[11] V. Kryachek, "Injection Moulding (Review)," *Powder Metallurgy and Metal Ceramics,* vol. 43, no. 7-8, pp. 336-348, 2004.

[12] A. Mannschatz, S. Höhn and T. Moritz, "Powder-binder separation in injection moulded green parts," *Journal of the European Society,* no. 30, pp. 2827-2832, 2010.

[13] D. Y. Park, Y. M. Oh, H. J. Hwang and S. J. Park, "An experimental approach to powder-binder separation of feedstock," *Powder Technology,* vol. 306, pp. 34-44, 2017.

[14] C. Quinard, J. Song, T. Barriere and J. Song, "Elaboration of PIM feedstocks with 316L fine stainless steel powders for the processing of micro-components," *Powder Technology,* vol. 2, no. 208, pp. 383-389, 2011.

[15] I. Kowalski and J. Duszczyk, "Specific heat of metal powder-polymer feedstock for powder injection molding," *Journal of Material Science Letter,* vol. 17, no. 18, pp. 1417-1420, 1999.

[16] Y. P. Mamunya, "Electrical and thermal conductivity of polymers filled with metal powders," *European Polymer Journal,* vol. 38, no. 9, p. 1887, 2002.

[17] V. Demers, S. Turenne and O. Scalzo, "Segregation measurement of powder injection molding feedstock using thermogravimetric analysis, pycnometer density and differential scanning calorimetry techniques," *Advanced Powder Technology,* no. 26, pp. 997-1004, 2015.

[18] H. He, Y. Li, J. Lou, D. Li and C. Liu, "Prediction of density variation in powder injection moulding-filling process by using granular modelling with interstitial power-law fluid," *Powder Technology,* no. 291, pp. 52-59, 2016.

[19] Z. Q. Cheng, T. Berriere, B. S. Liu and J.-C. Gelin, " A vectorial algorithm with finite element method for prediction of powder segregation in metal injection molding," *International Journal for Numerical Methods in Fluids,* vol. 70, no. 10, pp. 1290-1304, 2012.

[20] W. Fang, X. B. He, R. J. Zhang, S. D. Yang and X. H. Qu, "The effects of filling patterns on the powder-binder separation in powder injection molding," *Powder Technology,* vol. 256, pp. 367-376, 2014.

[21] S. D. Yang, W. Fang, Y. H. Chi, D. F. Khan, R. J. Zhang and X. H. Qu, "Bulk observation of aluminum green compacts by way of X-ray tomography," *Nuclear Instruments and Methods in Physics Research B*, no. 319, pp. 146-153, 2014.

[22] S. D. Yang, R. J. Zhang and X. H. Qu, "X-ray analysis of powder-binder separation during SiC injection moulding process in L-shaped mould," *Journal of European Ceramic Society*, no. 35, pp. 61-67, 2015.

[23] S. Yang, R. Zhang and X. Qu, "X-ray tomographic analysis of powder-binder separation in SiC green body," *Journal of the European Ceramic Society*, vol. 33, no. 15-16, p. 2935–2941, 2013.

[24] C. T. C. Crombie and D. C. Blaine, "Thermo-Gravimetric Analysis and Debinding Study of Powder Injection Moulded Titanium Alloy," in *AMI Light Metals Conference 2014*, Pilanesberg, 2014.

[25] G. Aggarwal, I. Smid, S. J. Park and R. M. German, "Development of niobium powder injection molding. Part II: Debinding and sintering," *International Journal of Refractory Metals & Hard Materials*, no. 25, pp. 226-236, 2007.

[26] M. Jenni, R. Zauner and J. Stampfl, "Measurement Methods for Powder Binder Separation in PIM," in *Euro PM2009 Proceedings*, Copenhagen, 2009.

[27] B. Hausnerova and D. P. P. Sanetrnik, "Surface Structure Analysis of Injection Molded Highly Filled Polymer Melts," in *Times of Polymer & Composites*, Ischia, 2013.

[28] Z. Y. Liu, N. H. Loh, S. B. Tor and K. A. Khor, "Characterization of powder injection moulding feedstock," *Material Characterization*, vol. 49, no. 4, pp. 313-320, 2003.

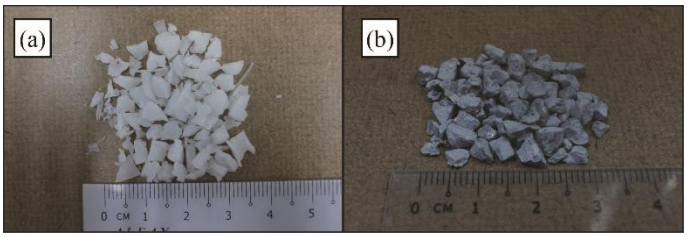

Fig. 1

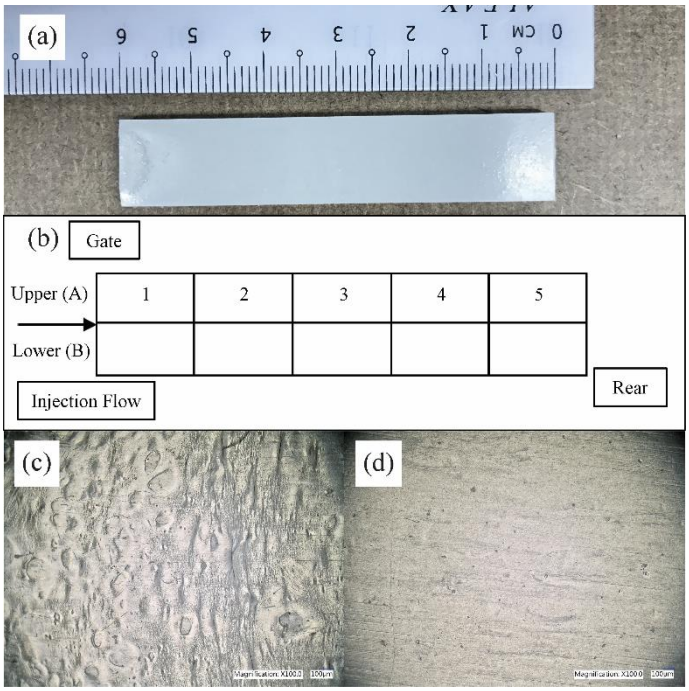

Fig. 2

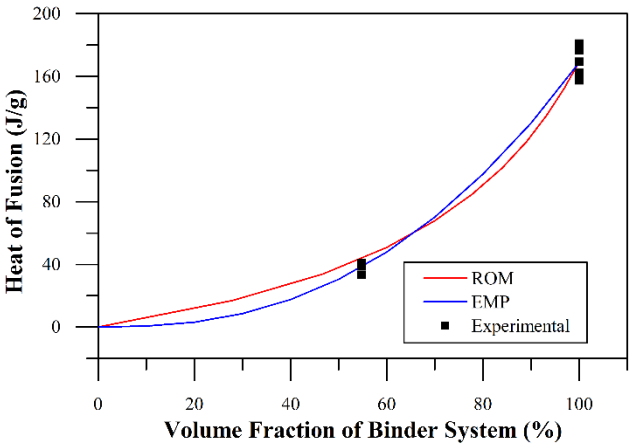

Fig. 3

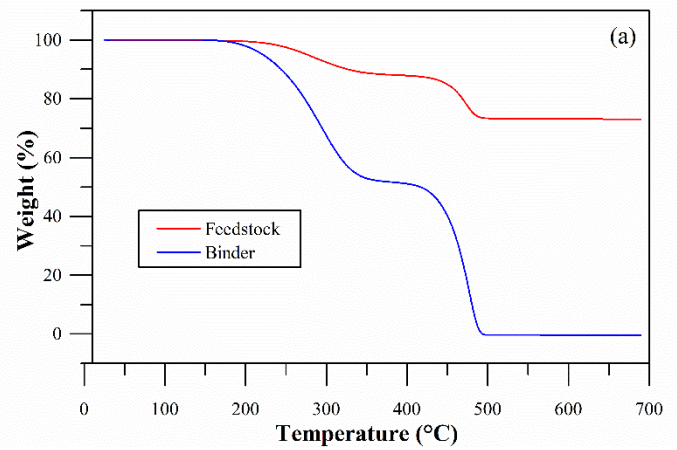

Fig. 4a

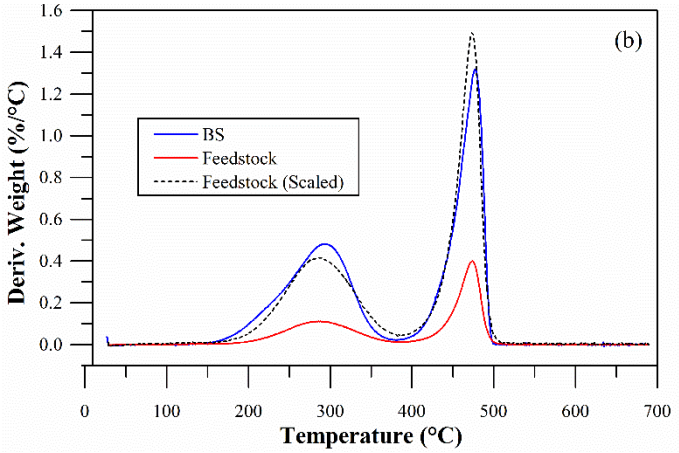

Fig. 4b

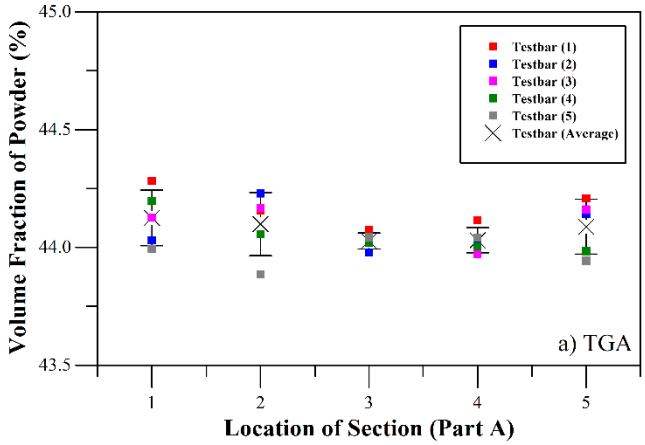

Fig. 5a

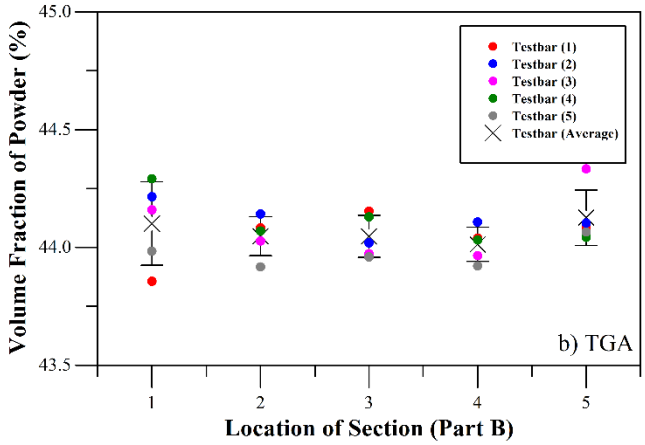

Fig. 5b

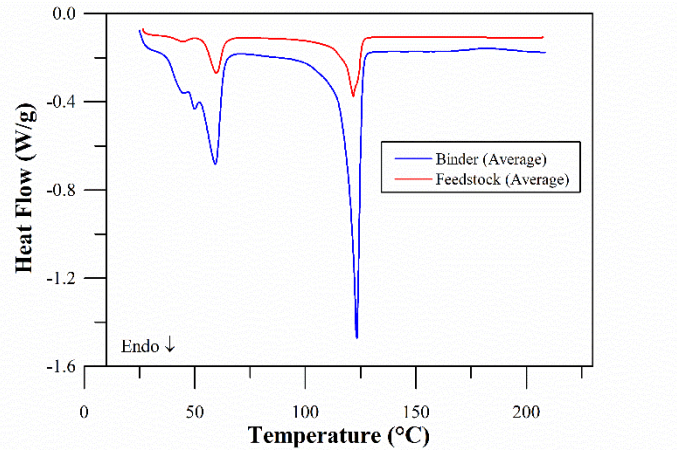

Fig. 6

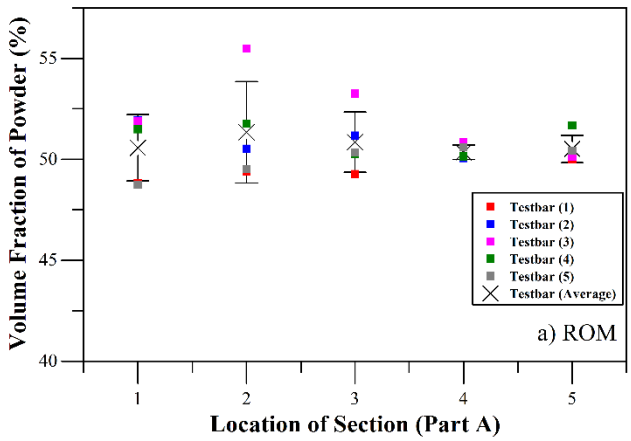

Fig. 7a

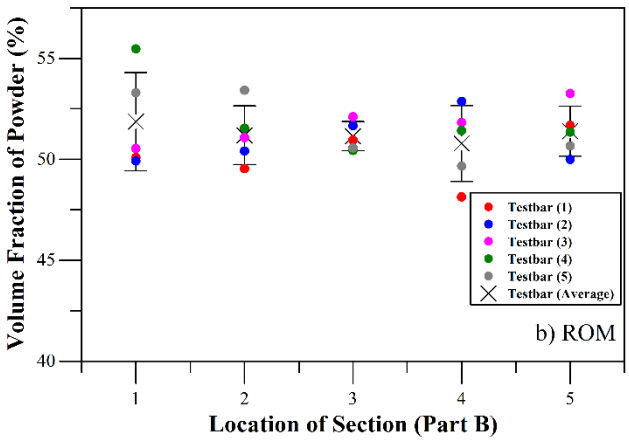

Fig. 7b

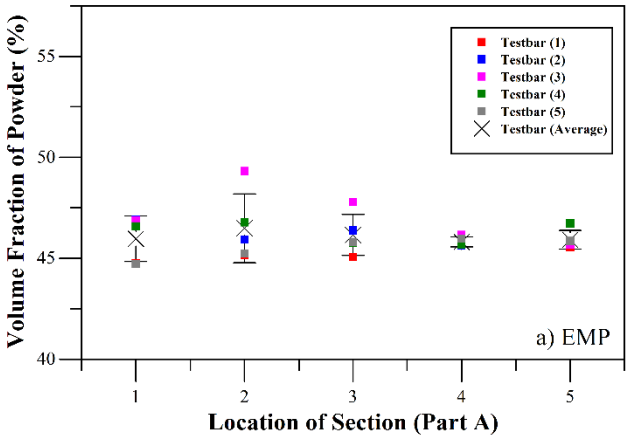

Fig. 8a

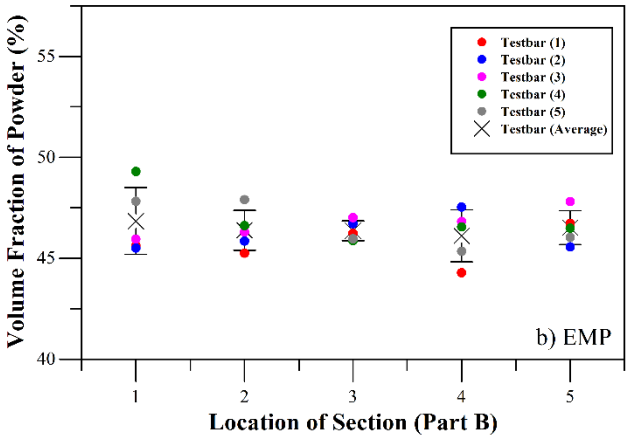

Fig. 8b

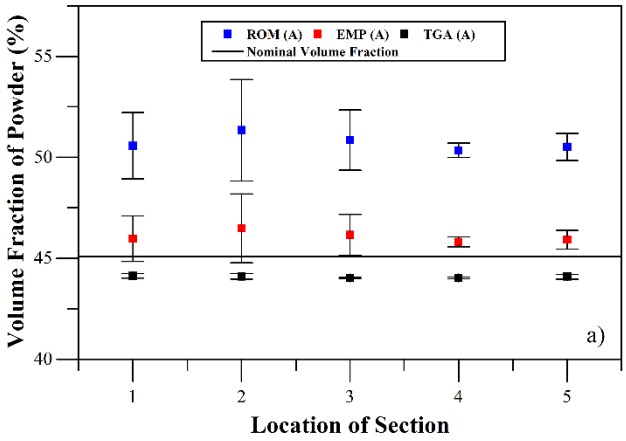

Fig. 9a

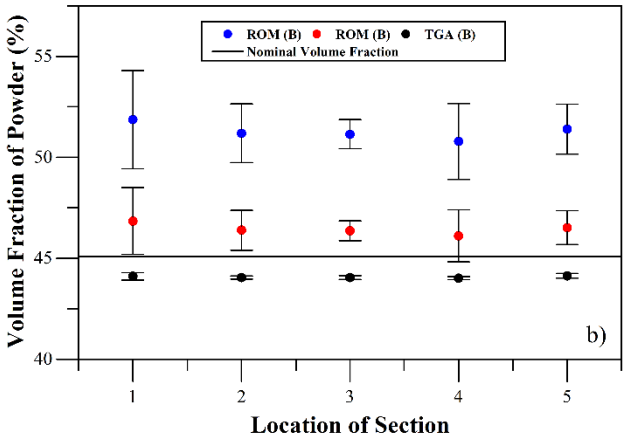

Fig. 9b

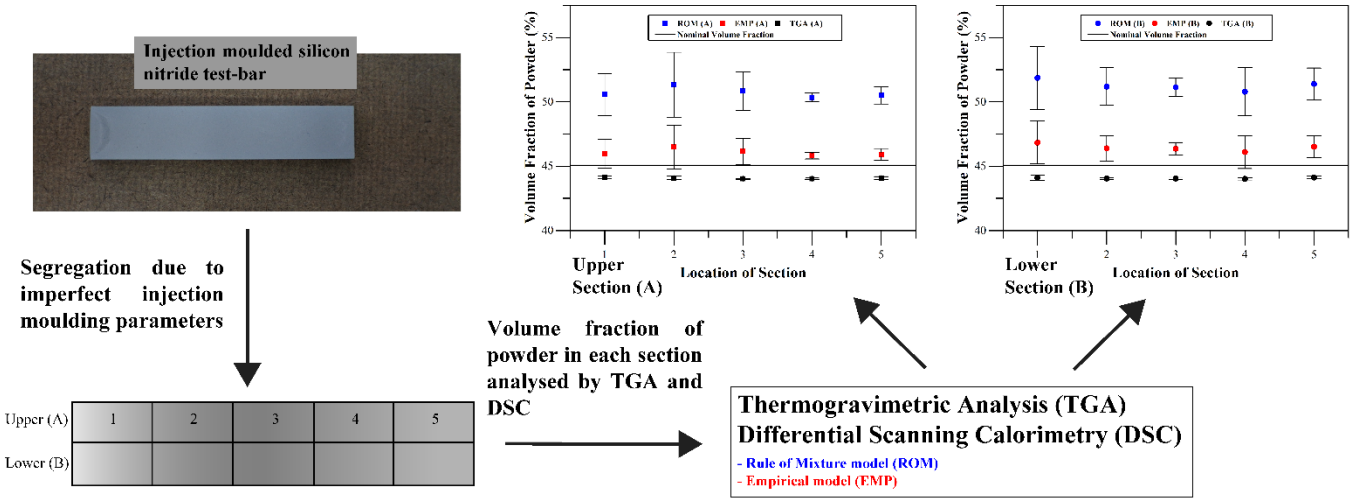

Graphical abstract

Highlights

- Variation in volume fraction of powder was measure on ceramic-based PIM feedstock.
- Segregation in green bodies can be measured by TGA with variations of 0.177 vol%
- Segregation in green bodies can be measured by DSC with variations of 1.710 vol%
- TGA is suitable for measuring the powder fraction in ceramic green bodies
- DSC empirical model is less accurate when compared to TGA, but it is 3 times faster